A Structural Model of Hydrophobically Modified Urethane−Ethoxylate (HEUR) Associative Polymers in Shear Flows

K. C. Tam,*,† R. D. Jenkins,‡ M. A. Winnik,§ and D. R. Bassett||

School of Mechanical and Production Engineering, Nanyang Technological University, Nanyang Avenue, Singapore 639798, Republic Of Singapore, Technical Center, Union Carbide Asia Pacific, Inc., 16 Science Park Drive, The Pasteur, Singapore 118227, Department of Chemistry, University of Toronto, Toronto, Ontario M5S 3H6, Canada, and UCAR Emulsions Systems Research and Development, Union Carbide Corporation, Cary, North Carolina 27511

Received January 30, 1998; Revised Manuscript Received April 27, 1998

ABSTRACT: This paper describes the rheological behavior of a HEUR (hydrophobic ethoxylated urethane) associative polymer with $C_{16}H_{33}$ end groups at 2.0 wt % concentration in aqueous solution. Under normal steady shear, this solution exhibits Newtonian behavior at low shear rates and, as the shear rate is increased, passes through a shear-thickening region before exhibiting a sharp decrease in viscosity. Here we report superposition-of-oscillation experiments on steady-shear flows to examine the state of the network structure under different shear conditions. The technique involves applying a steady shear deformation to the fluid, and once the steady state is achieved, a small amplitude oscillation is imposed on the sample to measure the linear viscoelastic properties. We observe that within the shear-thickening region, the plateau modulus is larger than in the Newtonian region, suggesting that shear-thickening is the result of a shear-induced increase in the density of mechanically active chains, which may be due to incorporation of free micelles or higher aggregates into the network structure. In the shear-thinning region, the Maxwell relaxation time decreases with increasing shear stress or shear rate. Thus shear thinning is a consequence of a shear-enhanced exit rate of the hydrophobic end groups from the micellar junctions of the network. This is the first experimental evidence for shear enhancement of the relaxation rate of an associative polymer network.

Introduction

Water-soluble polymers with hydrophobic substituents play important roles as thickeners and viscosity modifiers in a variety of water-borne technologies including paints, inks, and cosmetics. Early experiments on associative polymers examined commercial polymers and fully formulated mixtures. Much of our recent understanding of the behavior of these associative polymers (AP's) in aqueous solution comes from the study of model polymers in water in the absence of other formulation ingredients. The initial rationale for these experiments was the belief that a thorough investigation of the rheological properties of model associative polymers of known structure should reveal considerable insight into the association mechanism. Interest in model polymers began with the pioneering work of Jenkins,[1] who carried out systematic studies on a series of relatively well-defined HEUR (hydrophobic ethoxylated urethane) associative polymers. This type of polymer is prepared by chain extending a poly(ethylene glycol) (PEG) oligomer of narrow molecular weight distribution (MWD) with a diisocyanate and end-capping the product with a long chain alcohol. Because the chain extension process involves a condensation reaction, the final HEUR polymer has a broad MWD. Jenkins examined a series of HEUR polymers of molecular weight 16 000−100 000 with dodecyl or hexadecyl end groups and reference polymers without a hydrophobic end group.

HEUR associative polymers have been studied subsequently by many research groups.[1−12] Over the past several years, several key publications describing the rheology of HEUR polymers in aqueous solution have appeared.[1,3−5,8,10,11,13,14] The most interesting feature of all these experiments is that the viscoelastic properties of telechelic HEUR polymer solutions can be described in terms of the single element Maxwell model, consisting of a single elastic component connected in series with a viscous element.[3,15] These results indicate that the relaxation process of these systems under shear is dominated by a single terminal relaxation time. This relaxation time depends primarily on the hydrophobe chain length but also depends to a lesser extent upon polymer concentration and the molecular weight of the polymer.[3]

Information about the structures formed by linear associative polymers with hydrophobic end groups has been provided by an extensive series of spectroscopy and scattering measurements, involving not only HEUR polymers but also simpler model polymers, telechelic PEG polymers of narrow MWD, with molecular weights ranging from 4000 to 35 000, with hydrocarbon or fluorocarbon end groups. Methods employed include fluorescent-probe experiments,[5,16,17] pulsed-gradient spin-echo (PGSE) nuclear magnetic resonance (NMR) measurements,[18−21] dynamic light-scattering measurements, and at high polymer concentrations, small-angle scattering (SAXS, SANS) experiments.[7]

Fluorescent probe experiments establish that these types of polymers associate through their end groups to form micellelike junctions.[22] At low polymer concentrations in water, when the chain ends are sufficiently hydrophobic, the polymers associate to form flower micelles[23] consisting of looped chains in which both end

* To whom correspondence should be addressed.
† Nanyang Technological University.
‡ Union Carbide Asia Pacific, Inc.
§ University of Toronto.
|| Union Carbide Corporation.

S0024-9297(98)00148-X CCC: $15.00
Published on Web 06/09/1998

groups occupy the same micelle. In these starlike micelles,[24] the PEG chains in the corona are stretched relative to the normal coil dimensions of a PEG chain in water. Since HEUR polymers normally have a substantial fraction of chains with only one hydrophobic substituent, the free ends lacking a hydrophobe do not participate in the association. In the flower micelles, these chains are free to dangle into the solution beyond the corona formed by the looped chains. At higher polymer concentrations, a secondary association process occurs, accompanied by the formation of bridges between adjacent micelles. As the polymer concentration is increased further, percolation structures are formed that span the rheological cell and lead to a large increase in solution viscosity.

In the development of this picture of the association process, Annable et al.[3] contributed several key insights into the interpretation of the solution rheology. They identified the Maxwell relaxation time with the exit rate of the hydrophobe from the micelle-like junction. Simultaneously with the Winnik group, they put forward the idea of loop-to-bridge transitions in the buildup of the association structure with increasing polymer concentration, and of bridge-to-loop transitions accompanying structure breakdown during shear thinning under steady shear at elevated shear rates. In addition, they suggested that the concentration dependence of the relaxation time was due to the formation of superbridges in the system, an idea supported by recent simulations of polymer association.[13]

An interesting issue in our understanding of the association process is whether micelle formation by the polymer end groups follows a closed[6,16] or open association mechanism.[25] In closed association, an increase in polymer (hydrophobe) concentration leads to the formation of more micelles of identical size. Micelle size in these systems is best characterized by the term N_R, which describes the mean number of hydrophobic groups per micelle. In open association, the size of the micelles or association structures increases with increasing polymer concentration. For telechelic AP's, different views have been put forward, and the situation is relatively complex. A useful starting point is to consider the onset of association at low polymer concentration. HEUR systems are always characterized by a very broad onset of association as their concentration is increased, which may be due to their broad MWD.

When model telechelic associative polymer systems are characterized by a relatively high onset of association, which occurs in polymers containing weak hydrophobes compared to the length of the water-soluble polymer chain, the initial association appears to be an open process. The polymers associate into networks without passing through flower micelles. There is some limited evidence[17] to suggest that in these systems, once the network is formed, the micelle core size does not change very much. At very high polymer concentrations (>20 wt %), model telechelic polymers of narrow MWD (based upon PEG with *n*-alkyl ether end groups) form lyotropic cubic phases.[7] Low-angle X-ray and neutron-scattering measurements on the cubic phase indicate that the micelle junctions increase in size as the polymer concentration is increased further. In HEUR samples with strong hydrophobic end groups, careful fluorescence-quenching experiments indicate that flower micelle formation follows a closed association mechanism and that the micelle cores conserve their size over a significant range of relatively low polymer concentrations (<3 wt %). Xu et al.[4] and Yekta et al.[16] reported a mean end-group aggregation number of $N_R = 20$ for two HEUR polymers of molecular weights of 34 000 and 51 000 containing $C_{16}H_{33}$ end groups. These N_R values do not change with concentrations up to 3 wt %, where the system has rearranged to form extensive networks. There is some evidence for HEUR polymers that the mean number of hydrophobes per micelle core does not change with shear[26] or extensional flow.[27]

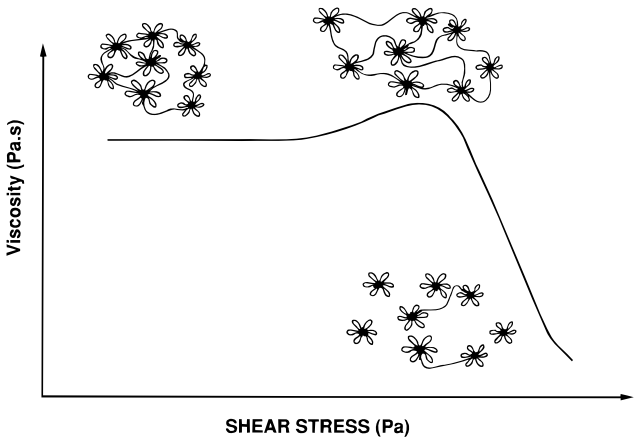

Figure 1. Viscosity versus shear stress of a HEUR polymer solution and the accompanying structure of the rosette micelles at the Newtonian, shear-thickening, and shear-thinning regions (after ref 16).

The shear-rate-dependent viscosity of a typical HEUR polymer solution is shown in Figure 1. In this figure, one observes a shear-rate-independent viscosity (Newtonian behavior) at low shear rates, shear thickening at intermediate shear rates, and severe shear thinning at elevated shear rates. Shear thickening is not very common in polymer solution rheology, but here the shear-thickening regime is strikingly prominent, particularly when one plots measured viscosity on a linear scale vs log shear rate, as shown in Figure 1. Several mechanisms have been proposed in the past to explain the observation of shear thickening.[28−31] These explanations are based on models that describe the effects of shear on the behavior of individual chains (non-Gaussian chain deformation) or shear effects involving multiple chains such as shear-induced polymer association or aggregation including temporary network formation during shear.

In Figure 1, we include hypothetical structures suggested by Winnik and co-workers to describe the state of the system in the Newtonian, shear-thickening, and shear-thinning regions.[4,16] These structures come from the model proposed by Yekta et al.,[16] shown in Figure 2, to describe the structures formed by HEUR polymers with end groups sufficiently hydrophobic to form flower micelles. In this model, flower micelle formation at low polymer concentrations is a closed association, followed by an open secondary association to form larger structures. The large increase in viscosity in the system at polymer concentrations near 1 wt % is due to formation of a macroscopic network made up of bridged micelles, which, at least near the percolation threshold of the system, conserves the mean number of chain ends per micelle core. In this model, at moderate shear rates, the structure is deformed, accompanied by the stretching of the bridging chains. A further increase in the shear rates causes the bridging chains to fragment,

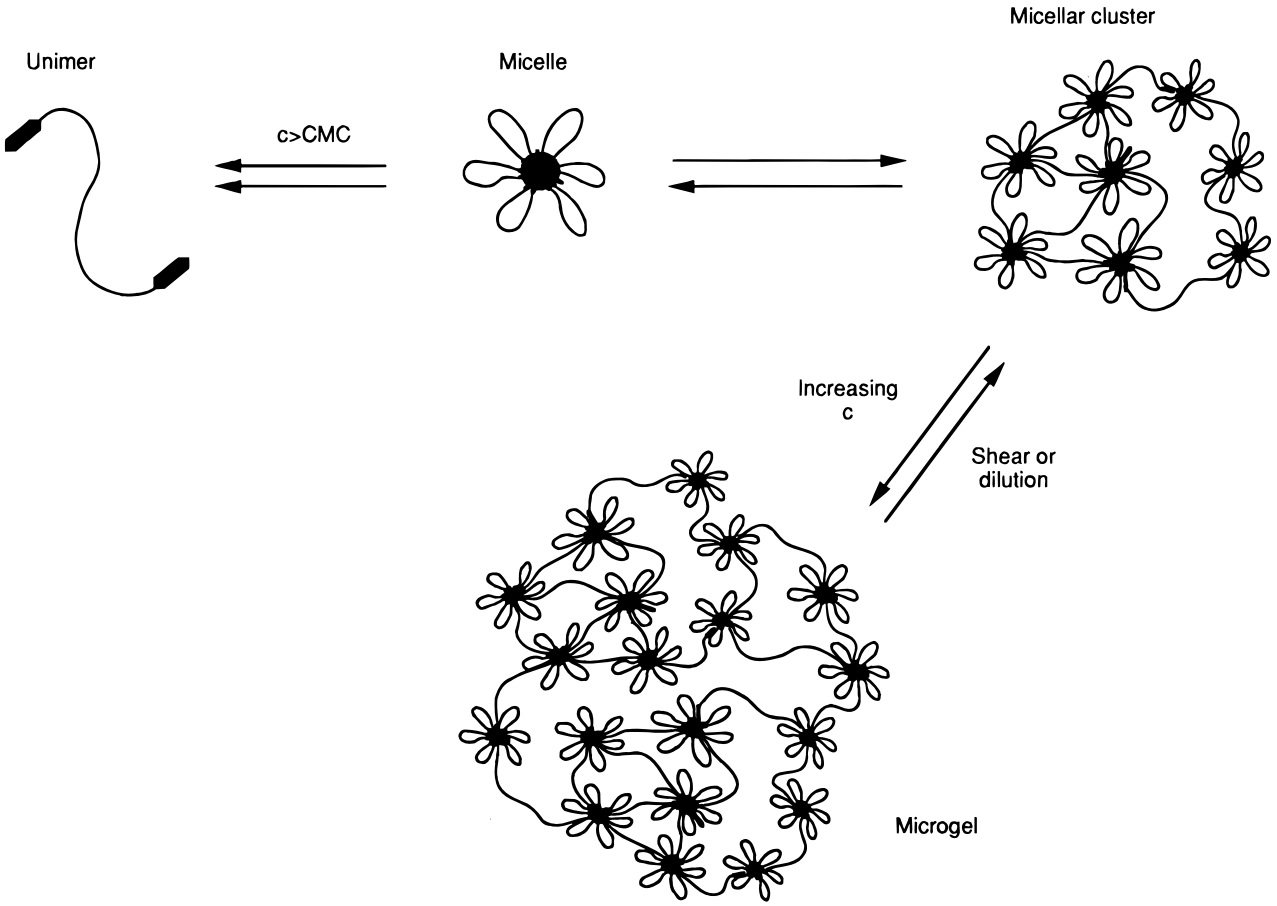

Figure 2. Schematic diagram depicting the microgel model for the HEUR structure in aqueous solution (after ref 6).

yielding smaller structures and discrete micelles. A large reduction in the viscosity is attributed to bridge-to-loop transitions, which conserves the number of micelle cores and their mean aggregation number N_R. And the structure drawn for the shear-thickening regime is intended to suggest non-Gaussian deformation of the chains in the network, as originally suggested by Jenkins.

Recently, we adopted the superposition of oscillations on steady-shear flow as a technique for investigating the structure of associative polymers.[32] In this technique, a continuous shear (or stress) is applied on a sample until a steady state is reached, at which time an oscillatory test is conducted to determine the viscoelastic behavior of the solution at a given shear or stress condition. This technique provides new and complementary information about the state of the network structure under various shear conditions, and this information is essential for evaluating structural models of the sort shown in Figure 2. This paper describes experiments employing the superposition of oscillations on the steady shear flow for the same HEUR associative polymer (sample AT22-3) examined by the Winnik group, for which the N_R values are known.

Experimental Section

The HEUR associative polymer, a urethane-coupled poly(oxyethylene) end-capped with $C_{16}H_{33}O-$ groups was supplied by Union Carbide. We refer to it as AT22-3, which is the nomenclature used in the Winnik group publications.[4,16] This sample has $M_n = 51\,000$, $M_w/M_n \sim 1.7$, and a degree of end functionalization of 1.7. The polymer was stored in the refrigerator at 4 °C to minimize air oxidation and subsequently used to prepare a 5 wt % stock solution using Millipore MilliQ distilled water. From the 5 wt % stock solution, a test solution of 2.0 wt % was prepared and kept in the refrigerator prior to testing.

The rheological properties of the 2.0 wt % AT22-3 solution was measured using a TA (Carrimed CLS500) controlled stress rheometer. Two different cones were used, a 4 cm diameter, 2° cone angle and 2 cm diameter, 0.5° cone angle. All experiments were conducted at 25 °C. Both steady-shear and oscillatory tests were conducted. For oscillatory testing, the strain was kept at less than 20% to ensure that the test is within the linear viscoelastic region. Parallel superposition of oscillation on steady-shear flows was conducted at various applied stresses or shear rates. A detailed discussion of the superposition technique, together with a schematic diagram depicting the stress and strain curves involved is reported elsewhere.[32]

Results and Discussion

Viscosity−Shear Stress Profile. The viscosity/shear stress data for a 2.0 wt % AT22-3 solution is shown in Figure 3. The magnitude of the zero shear viscosity is about 5.5 Pa•s, which agrees reasonably well with data obtained by Jenkins[1,2] and by the Winnik group.[4] In this report, we prefer to plot viscosity vs shear stress, since the viscosity data show a more distinct dependence on shear stress than on shear rate. As shown in Figure 3, the solution exhibits a constant viscosity up to an applied stress of 20−25 Pa, where the onset of shear thickening is observed. This thickening behavior persists until 170−180 Pa. Beyond this stress level, a dramatic decrease in the viscosity is observed. This decrease occurs within a small stress window ranging from 180 to 200 Pa. Over this stress range, the

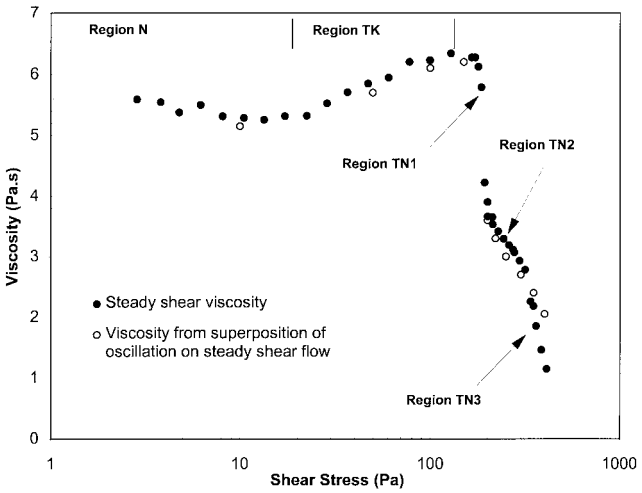

Figure 3. Plot of viscosity versus shear stress measured at 25 °C for AT22-3 at 2.0 wt % concentration.

solution undergoes a 50% drop in viscosity. When the applied stress is increased, two further transitions are observed, a more gradual decrease in viscosity at stress levels between 200 and 300 Pa, followed by another sharp decrease at higher shear stresses. In discussing this behavior, it is useful to classify the viscosity profile into distinct regions, as marked in Figure 3.

•Region N. Newtonian $\tau < 25$ Pa.

•Region TK. Shear thickening 25 Pa $< \tau <$ 180 Pa.

•Region TN1. First shear thinning: large drop in viscosity at 180 Pa $< \tau <$ 200 Pa.

•Region TN2. Second shear thinning: reduced slope in η vs τ profile 200 Pa $< \tau <$ 300 Pa.

•Region TN3. Third shear thinning: large drop in viscosity $\tau >$ 300 Pa.

It is unusual for polymer solutions to exhibit multiple and distinct shear-thinning regions. In previous studies of the rheology of HEUR associative polymers,[3,4,8,11] only Jenkins[1] reported the observation of changes in shear-thinning behavior at high-shear stress. Because of this unusual behavior, we were concerned that artifacts, such as fluid fracture, fluid instability, or some feature of cone geometry might affect the shape of the measured profiles at high-shear stress. To allay these concerns, we carefully examined the sample during testing but noted no fluid fracture or fluid exiting the sample cell. In addition, experiments were repeated with a different cone (2 cm and 0.5°), and essentially identical results were obtained. The smaller cone angle enabled the instrument to achieve higher shear rates at significantly lower rotational speeds. From the careful examination of the fluid during testing, we are satisfied that the viscosity profile as shown in Figure 3 represents the material properties of the polymer solution. The data in Figure 3 indicate that the behavior of the polymer under shear is more complex that depicted in the Winnik model.

Superposition of Oscillations on Shear Flows. Our instrument allows us to examine samples in which oscillatory shear is superimposed upon a system experiencing a steady-shear deformation. In these experiments, one applies a stress or a shear gradient on the sample until the steady state is achieved. At this point an oscillatory test is superimposed onto the sheared sample, and the linear viscoelastic properties are measured over a wide range of frequencies, ranging from 0.1 to 200 rad/s. Using these techniques, as described

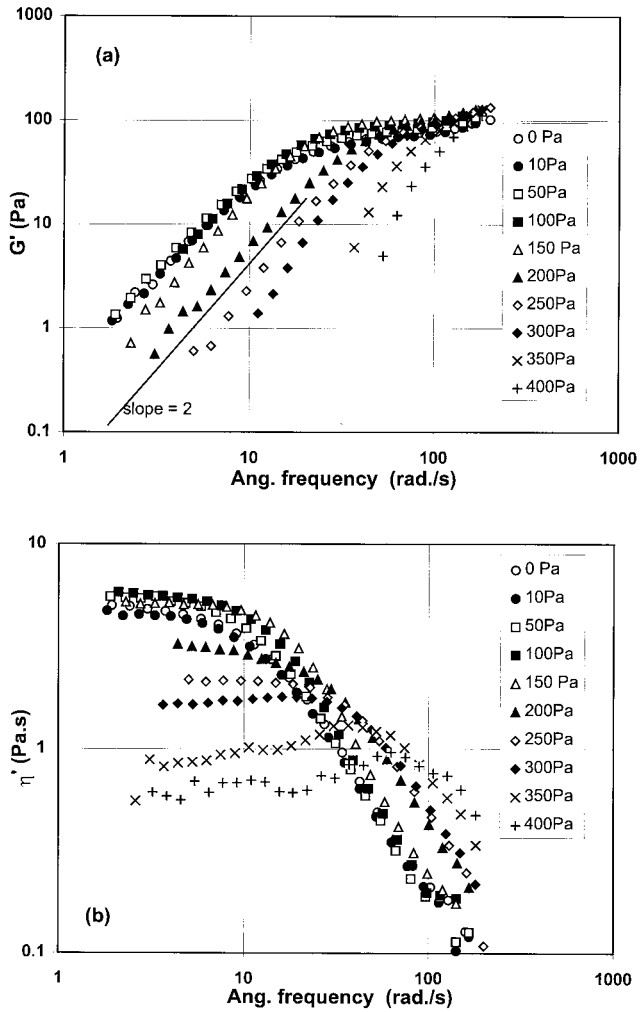

Figure 4. Linear viscoelastic properties of 2.0 wt % AT22-3 at 25 °C: (a) storage moduli; (b) dynamic viscosity. Measurements were conducted at applied stresses of 0−400 Pa using the parallel superposition techniques.

recently by Tirtaatmadja et al.,[32] we hope to be able to probe the structural behavior of the polymer network under different shear conditions. This would, for example, allow us to examine whether shear thickening results from chain or network deformation or whether it is a consequence of the formation of an increased number of junctions in the system. These experiments might also allow further insights into the suggestion both by the Winnik group[4,16] and by Richey et al.[26] that during shear thickening and the early stages of shear thinning, the mean end-group association number of the network junctions remains constant. The steady-shear viscosity at each of the applied stresses obtained from the superposition experiments was superimposed onto the steady-shear viscosity profile in Figure 3, and good agreement was observed.

In Figure 4a we plot values of the storage modulus vs frequency at applied stress levels ranging from 0 to 400 Pa. Corresponding values of dynamic viscosity are presented in Figure 4b. At applied stresses of up to 25 Pa, both the storage modulus and the dynamic viscosity remain essentially constant and have the same magnitude as that of the solution without applied stress. At this level of stress, the shear viscosity remains in the limiting low-shear Newtonian regime, where the response of the network to the oscillatory frequency is faster than the imposed shear rate. These results

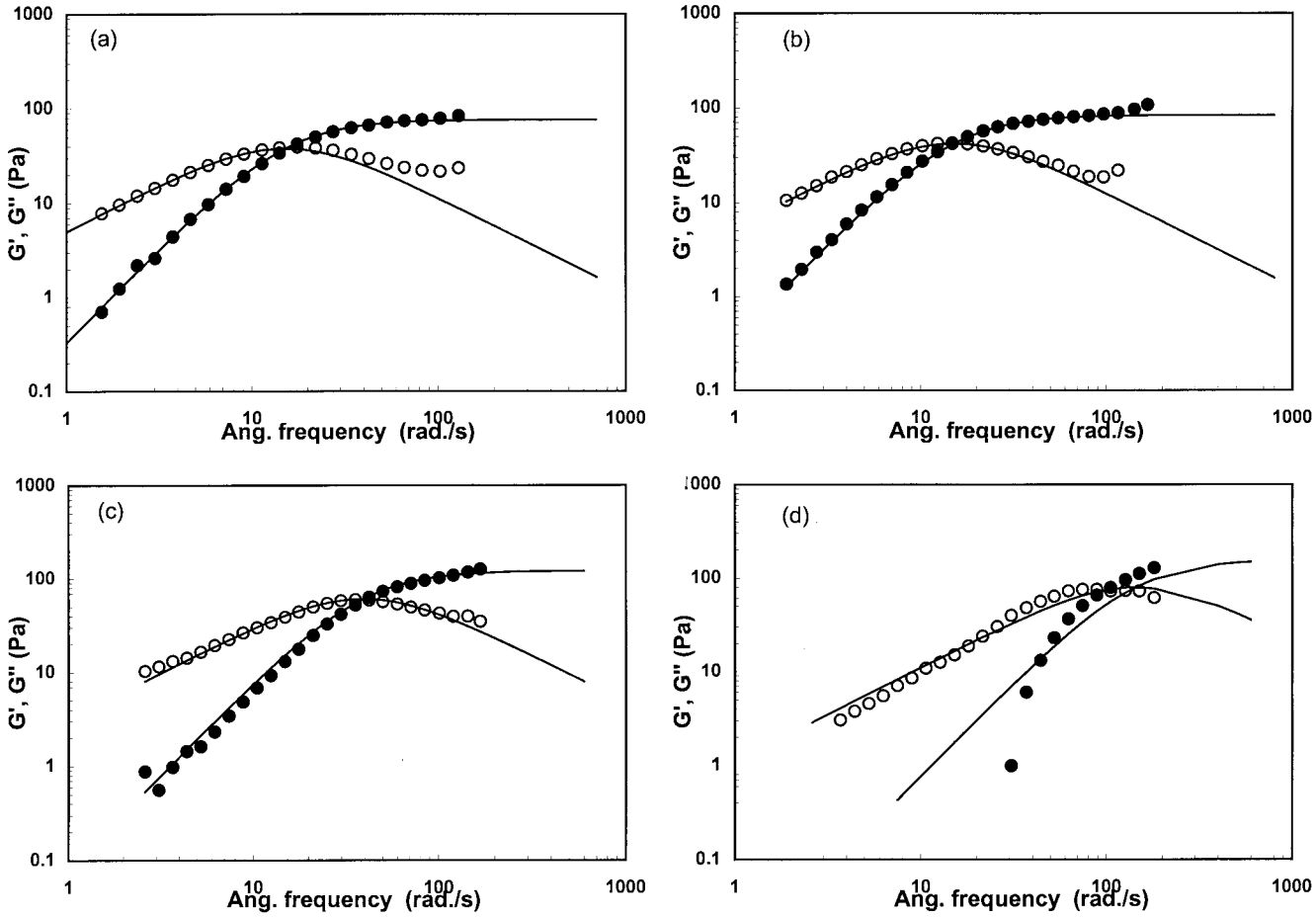

Figure 5. Fitting of Maxwell model to the dynamic properties of 2.0 wt % AT22-3 at various applied stresses: (a) no applied stress; (b) applied stress = 50 Pa; (c) applied stress = 200 Pa; (d) applied stress = 350 Pa.

also indicate that there is no steady-shear-imposed change in the structure of the network.

Our first important new results appear in the shear-thickening region (25 Pa < τ < 180 Pa). Here we observe that both the storage modulus and dynamic viscosity increase, reaching a maximum that corresponds to the upper viscosity limit of the shear-thickened viscosity profile. The data at each of the applied stresses were fitted to the single-mode Maxwell model, as described by eqs (1) and (2). The Maxwell

$$G'(\omega) = \frac{G_0\omega^2\lambda^2}{1 + \omega^2\lambda^2} \tag{1}$$

$$G''(\omega) = \frac{G_0\omega\lambda}{1 + \omega^2\lambda^2} \tag{2}$$

model is a two-parameter model in which the storage and loss moduli at all frequencies ω can be described in terms of a plateau modulus G_0 and a terminal relaxation time λ.

The data are plotted in Figure 5a−d, where the solid lines represent the best fits to the model using the Maxwell equations (1) and (2). In previous work, good fits of the data to these expressions were found at zero applied stress. Here we find good fits to the data for applied stresses ranging from zero to about 300 Pa, corresponding to the maximum of the viscosity profile before a large decrease in the viscosity is observed. At higher applied stresses, however, where the viscosity starts to decrease significantly, the simple single-element Maxwell model is less able to describe the viscoelastic behavior of the solution.

In fact, the overall behavior is more subtle. The dynamic viscosity increases with applied stress, reaches its maximum value at ca. 100 Pa, and then decreases as the applied stress is further increased. The plateau modulus, in contrast, increases with applied stress, and reaches its maximum value at a value of 180 Pa. At higher levels of applied stress, where the solution begins to exhibit shear thinning, the plateau modulus remains high. At these stress levels, however, the plateau modulus cannot be determined accurately, because the viscoelastic data deviate more and more from the behavior expected of a simple Maxwell-type fluid. However, we can estimate the magnitude of the plateau modulus using the expression $G_0 = \eta_0/\lambda$.

Another widely used method of examining the suitability of the Maxwell model in describing the viscoelastic properties of polymer solutions is to present the data in the form of a Cole−Cole plot. The mathematical expression for the Cole−Cole plot can be derived by rearranging equations (1) and (2) into the form given by eq 3:

$$G''(\omega) = [G'(\omega)G_0 - G'(\omega)^2]^m \tag{3}$$

where $m = 0.5$. Data that fit the Maxwell model yield a perfect semicircle when plotted in this way. One advantage of this method of examining the data is that the plateau modulus G_0 can be determined from the

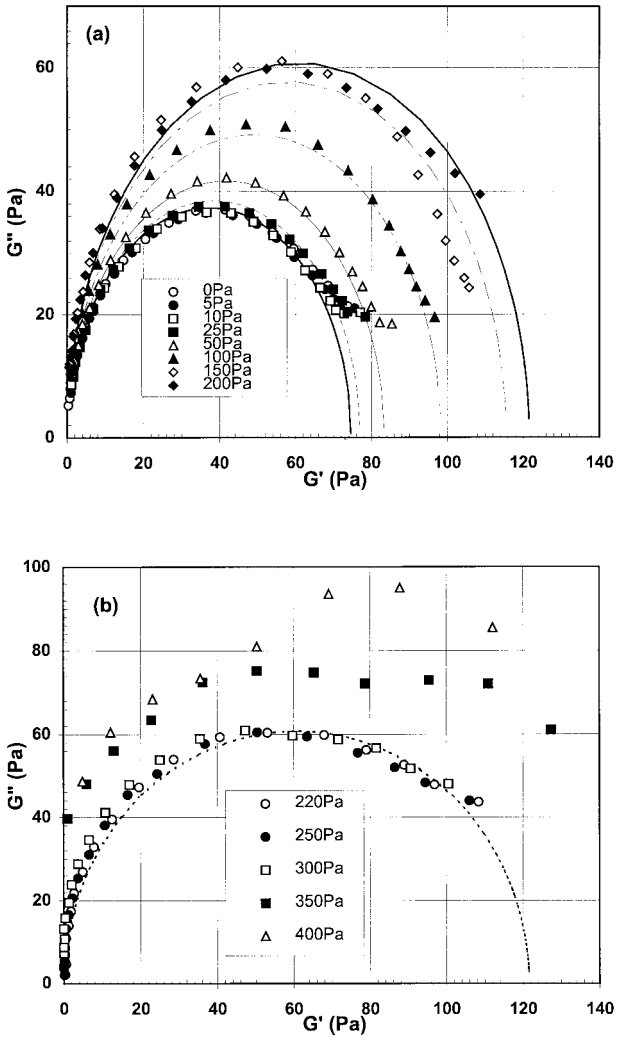

Figure 6. Cole−Cole plot of the dynamic properties of 2.0 wt % AT22-3 with the accompanying fitting of the Maxwell model shown in solid lines.

intersection of the semicircle with the horizontal *x*-axis. Cole−Cole plots of the linear viscoelastic data, at applied stresses ranging from 0 to 400 Pa, are shown in Figure 6a,b. It is evident from these plots that good fits are obtained for applied stresses up to ca. 300 Pa. Beyond this level, the fitting does not hold as well and hence the determination of the plateau modulus G_0 in this way is subject to some error. The results from the plots show very clearly that G_0 increases with applied stress up to about 200 Pa, it remains fairly constant up to ca. 300 Pa, and beyond this, the magnitude of G_0 begins to decrease sharply.

The relaxation time λ also provides important information about the viscoelastic response of polymer solutions. This parameter can be obtained in several ways, by fitting the data to eqs 1 or 2, from the intersection of the G' and G'' curves, where the inverse of the frequency at the intersection point is equal to the relaxation time, or from the second-order region of the G' and G'' curves in terms of eq 4. A signature of data that fit the simple Maxwell model is that the relaxation times calculated by each of these different methods are identical.

$$\lambda = \frac{G'}{\omega^2 \eta_0} \tag{4}$$

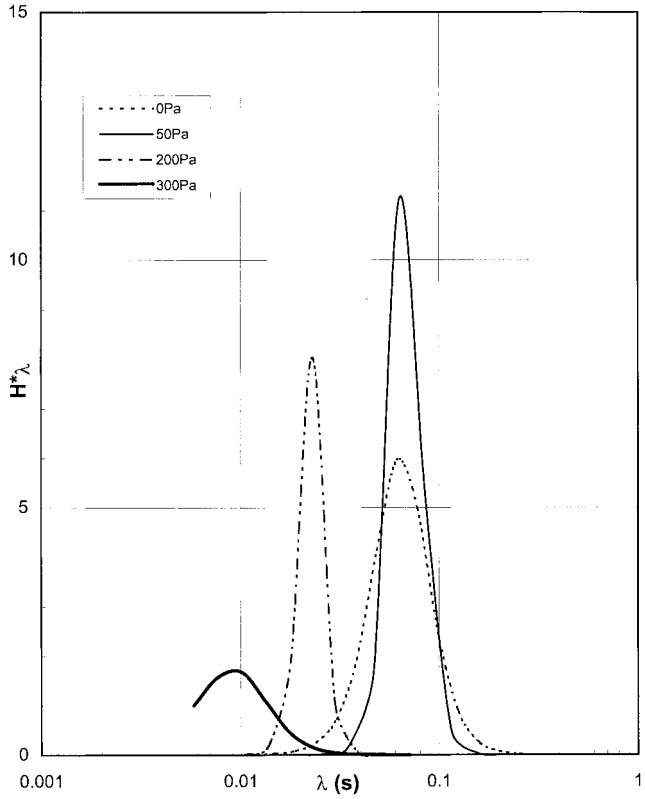

Figure 7. Mechanical relaxation time distributions of 2.0 wt % AT22-3 at an applied stress ranging from 0 to 300 Pa.

Relaxation times, λ obtained using the above methods are identical. In the present study, the relaxation times were obtained by fitting the data to eqs 1 and 2.

The viscoelastic response of the HEUR polymer at various applied stresses may be more clearly depicted by examining the distribution of relaxation times. Information on the relaxation spectrum $H(\lambda)$ can be derived from data obtained in the frequency domain according to the expressions below:

$$G'(\omega) = \int_{-\infty}^{\infty} H(\lambda)\left[\frac{\omega^2\lambda^2}{1+\omega^2\lambda^2}\right] \mathrm{d}(\ln \lambda) \tag{5}$$

$$G''(\omega) = \int_{-\infty}^{\infty} H(\lambda)\left[\frac{\omega\lambda}{1+\omega^2\lambda^2}\right] \mathrm{d}(\ln \lambda) \tag{6}$$

The calculation of the relaxation spectrum from material functions such as storage and loss modulus requires the inversion of the type of equation as shown in eqs 5 and 6. It is well-known that inversion of such integral equations results in an unstable problem. Various numerical techniques have been developed, most of them based on the regularization method, to solve the ill-posed problem as given by eqs 5 and 6. An algorithm called NLREG developed by Honerkamp and Weese[33] and commercialized by Haake (POLYSOFT software) was used to calculate the relaxation time spectrum. The method is based on a nonlinear regularization technique, which is capable of determining the multimode relaxation time spectrum. The spectra obtained from the storage and loss modulus at various applied stress conditions are plotted as $H(\lambda)\lambda$ vs λ in Figure 7. The results show that the relaxation time distribution for the system in the absence of applied stress is reasonably narrow, with a mean relaxation

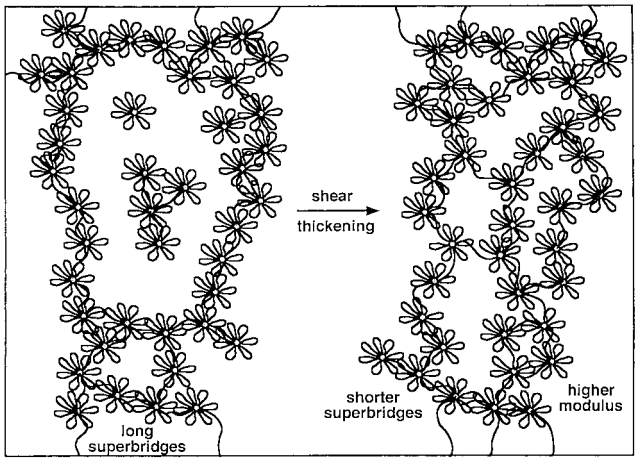

Figure 8. Structural model of the HEUR at the shear-thickening region. The model depicts the incorporation of unassociated rosette micelles into the superbridge network coupled with the rearrangement of the superbridges to yield a net increase in the number of junctions.

time of 0.065 s. In the shear-thickened region (applied stress ca. 50 Pa), not much change in the mean value of λ is observed. However, an interesting feature of the system is that the relaxation time distribution has narrowed compared to that at no applied stress, suggesting that the size distributions of micellar clusters have narrowed somewhat. In the second shear-thinning region (TN2), one observes that the relaxation spectrum has sharpened considerably compared to that at an applied stress of 50 Pa. Moreover, the mean relaxation time has shifted significantly to a lower value of 0.02 s. In the third shear-thinning region, when the applied stress reaches 300 Pa, the distribution of relaxation times is broadened and shifted to shorter times, leading to a decrease in the mean λ value.

Relating Maxwell Behavior to Molecular Properties. Using the superposition of oscillation on steady-shear flows, we are able to measure the effects of applied stress on the dynamic viscosity, the plateau modulus and the Maxwell relaxation time. This behavior is compared with the effects of applied stress on the steady shear viscosity, as shown in Figure 3. We note first that the dynamic viscosity follows the same trend as the steady shear viscosity profile. Shear thickening occurs at applied stresses of 10−100 Pa, and beyond this, the dynamic viscosity decreases with increasing applied stress.

Plateau Modulus. In terms of the simple theory of rubber elasticity, as extended to transient networks by Green-Tobolsky,[34] the magnitude of the plateau modulus is proportional to the number density ν of mechanically active chains in the network,

$$G_0 = \nu RT \tag{7}$$

Our observation of an increase in the plateau modulus in the shear-thickening regime is the first evidence that shear thickening occurs because of a rearrangement of the network to create more junctions. The applied stress induces a change in the relative population of looping chains and bridging chains, i.e., stress-induced loop-to-bridge transitions that would lead to an increase in the number of junctions but preserve the mean end-group aggregation number of the junctions.[4,16,27,35]

Both Annable et al.[3] and Groot and Agteroff[13] have discussed the role of "superbridges", or long linear,

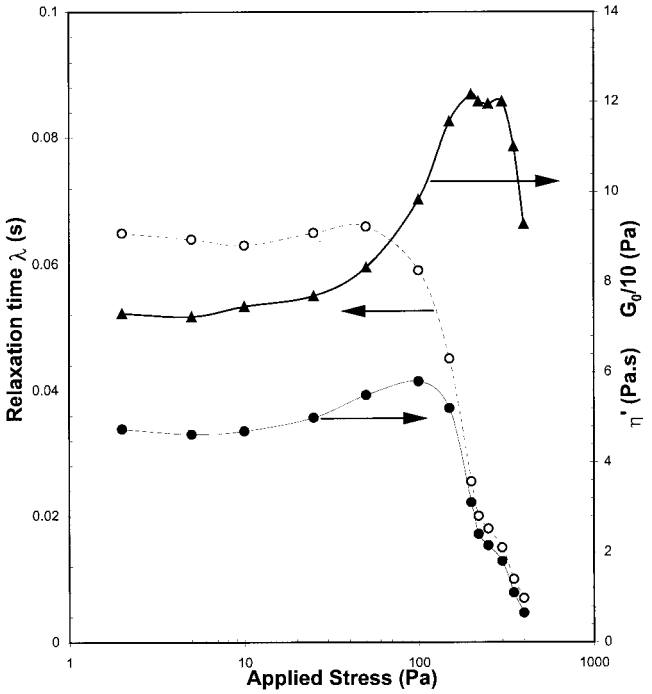

Figure 9. Plot of relaxation time (λ) (○), dynamic viscosity (η') (●), and the plateau modulus (G_0) (▲) versus applied stress for 2.0 wt % AT22-3 solution.

mechanically active, sequence of connections that are part of the percolation networks that provide mechanical connectivity between the cone and plate in the sample cell. Superbridges in solutions of AT22-3 consist of a string of micelles (with two bridging chains each) connected to a more extensive network of micelles at either end. At the concentration of 2 wt %, it was determined that $G/RT \ll D^{-3}$ or n (where D is the diameter of a flower micelle and n is the number of flower micelles); hence superbridges are deemed to exist. This was further supported by the work of Annable et al.[36] For the concentration of polymer examined here (2 wt %), we expect that not all micelles would be incorporated into the percolation network. We present a pictorial view of this process in Figure 8. Stress-induced loop-to-bridge transitions that increase the fraction of micelles included in the mechanically active network decrease the mean length of the superbridges. The process depicted in Figure 8 takes place at a concentration above the overlap concentration of free flower micelles, i.e., in a solution completely filled with associated polymer structures: individual flower micelles, larger aggregates, and a percolation network of bridged micelles. Thus the empty spaces in Figure 8 should be thought of as filled with finite aggregates that do not contribute to the plateau modulus at this concentration of polymer.

We summarize our results on the shear-stress dependence of the plateau modulus in Figure 9. Here one sees that at the onset of shear thickening, the plateau modulus increases from 70 to about 120 Pa. It reaches its maximum value at an applied stress of 200 Pa and then remains constant over a limited applied stress window. However, at applied stresses greater than ca. 300 Pa, a substantial decrease in the plateau modulus is observed. The values of G_0 at applied stresses greater than 300 Pa are estimated from the expression $G_0 = \eta/\lambda$, where the values of η are obtained from the steady-shear curve (Figure 3) and values of λ from the oscil-

latory data at an applied stress of 300−400 Pa (Figure 4). Taken together, these results indicate that the enhanced number of mechanically active chains created in the shear-thickening regime persists into the first two shear-thinning regimes, TN1 and TN2. Only at applied stresses greater than 300 Pa does the network fragment to yield smaller, finite structures. Although this type of network fragmentation is suggested in the model shown in Figure 2, it does not accommodate the subtle variety of changes that occur in the three shear-thinning regimes.

Relaxation Times. A system that exhibits simple Maxwell rheological behavior is characterized by a single relaxation process that dominates the response of the system to stress. Annable et al.[3] have explained this behavior by pointing out that the dominant relaxation process in these end-capped systems is the exit of a hydrophobic group from a junction point. They compared exit rates and binding energies of surfactants in micelles to the relaxation times and activation energies for the viscosities of HEUR systems and found close correspondence. They tested this idea by carrying out an important experiment in which they examined mixed systems containing two or three HEUR associative polymers (APs) with different hydrophobic end groups and found well-defined relaxation times that corresponded to those of the individual APs. The beauty of this explanation is that it provides a coherent explanation of the solution rheology in terms of the molecular behavior of its components.

Our experiments provide information about changes in the Maxwell relaxation time as a function of applied stress and allow us to quantify the connection between the molecular processes described above and theories of the response of transient networks to shear. In terms of the transient network theory proposed by Jenkins[1] and Tanaka and Edwards,[10] the exit rate of a chain end from a junction can be described by an expression of the form

$$\lambda^{-1} = \beta \exp(-E_m/RT) \tag{8}$$

where E_m is the potential barrier to disengagement of a chain end from a junction point, which may, in the systems examined here, be equated to the binding energy of the hydrophobe to its micelle. In eq 8, β is a shear-dependent prefactor that couples the energy of chain deformation to an enhanced "pull-out" rate of the chain from its junction. For a HEUR polymer similar to that of AT22-3, Annable et al. determined a value of $E_m \sim 70$ kJ/mol from the temperature dependence of the solution viscosity. In terms of our experiments, the application of a stress in excess of 100 Pa causes the chains in the network to stretch and provides the additional energy needed to overcome the potential barrier for disengagement.

In Figure 9 we observe that the relaxation times follow the same trend as the viscosity, exhibiting a small increase with applied stress over the lower end of the shear-thickening region. The onset of the decrease in λ occurs at a somewhat lower stress than the maximum of the dynamic viscosity in the shear-thickening region. We find a sharp decrease in λ over the applied stress range of 50−200 Pa, but beyond this stress level, the decrease is less pronounced. Our results indicate, as predicted by transient network theory, that the exit rate of the hydrophobe depends on the applied stress and is enhanced by the application of stress.[3,37] Thus, we can conclude that over the region where the solution experiences a large drop in the viscosity, the origin of this effect is the shear-induced increase in the chain-end exit rate, which means that for mechanically active chains, the lifetime of a hydrophobe in a micelle is reduced. Shear enhancement of the relaxation rate has been observed for plastics[38] and gelatin gels.[39]

Over the shear-thickening region, other factors must operate, as the application of stress has the effect of increasing the relaxation time slightly, hence reducing the exit rate. Several explanations are possible. For example, as discussed above, we know that the network junction density increases over the shear-thickened region. An increase in the number of mechanically active chains may be responsible for distributing the imposed stress and hence reducing its effect on the micellar core or cluster. Alternatively, changes in the fraction of bridging vs looping chains may affect the configurational entropy of the chains in the corona of each micelle. This might serve to offset the effect of the imposed stress on the deformation free energy of the bridging chains. Finally, a decrease in the length of superbridges in the system would lead to a natural increase in the measured relaxation time of the system (cf., Figure 8). The earlier onset observed in the relaxation times at an applied stress of ca. 50 Pa could be due to the competing effects of enhanced exit rates of the bridging chains (which correspond to a lower λ) and the reduction in the length of the superbridges, which result in a higher λ. The results indicate that the latter contribution to the relaxation times at a higher applied stress is less significant than the increase in the exit rates of the bridging chains.

Thixotropy and Stress Relaxation. In the steady-shear experiments described above, we identify three distinct shear-thinning regimes that follow the onset of shear thickening. We would like to obtain additional information about the system in these shear-thinning regimes. A sensitive experiment to help identify the nature of the structures present within the network involves examining the recovery of the system from an imposed shear history. Such studies, which examine the thixotropic behavior of the system, can provide useful information about the rate of destruction of network structures following the application of stress and the rate of rebuilding these structures following removal of the stress. The result of this type of experiment is presented in Figure 10. In Figure 10a, we observe that when the stress is increased from 1 to 180 Pa (from the zero shear viscosity to the maximum viscosity in the shear-thickening regime), and then back to the starting point, the two curves are identical. This establishes that the deformation and the restoration of the structure is completely reversible and occurs faster than the experimental measurement time of about 10−11 min. In our second test (Figure 10b), the stress is increased from the Newtonian region at a stress of 5 Pa to region TN2 at a stress of 300 Pa, and then the stress is decreased back to the Newtonian region. As the stress is decreased from 300 to 100 Pa, a lower viscosity is observed, indicating hysteresis over this region. However, as the stress is further reduced from 100 to 5 Pa, an identical viscosity curve is obtained. This suggests that the starting and final structures of the sample after undergoing the deformation at an applied stress range between 5 and 300 Pa are essentially

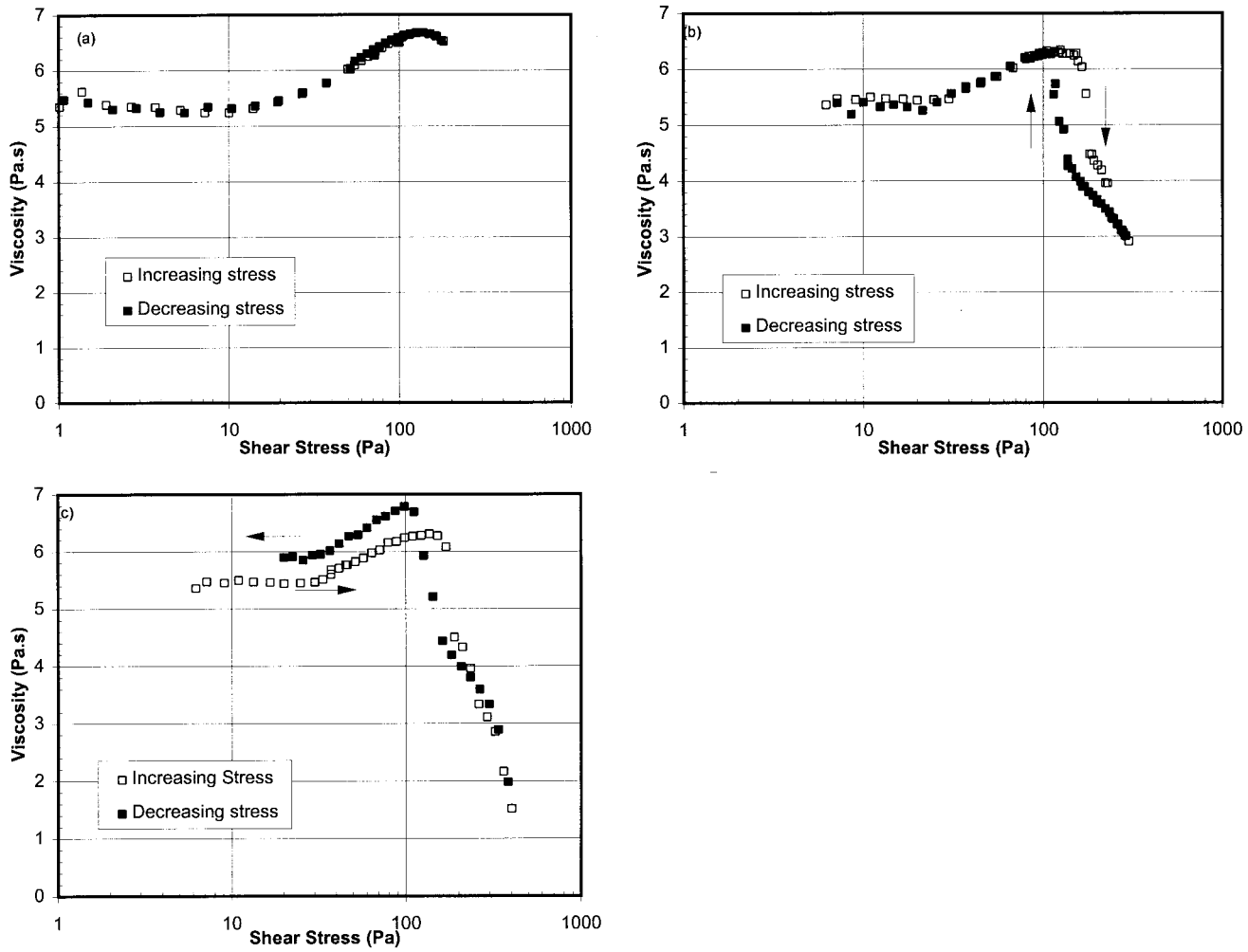

Figure 10. Thixotropic flow curves of 2.0 wt % AT22-3 solution at various applied stresses: (a) applied stress of 1−180 Pa; (b) applied stress of 6−300 Pa; (c) applied stress of 6−400 Pa.

identical. However, as the applied stress is increased further to 400 Pa (Figure 10c), the viscosity curve of the decreasing applied stress is not the same. Hysteresis is evident over the entire stress range, and the magnitude of the viscosity in the low-shear Newtonian region is higher.

The hysteresis observed after the system is subjected to a shear stress of 300 Pa indicates that the global relaxation of the solution structure occurs on a longer time scale than that of the measurement for shear stresses decreasing from 300 to 100 Pa, whereas further reduction in the applied stress leads to rapid recovery of the initial structure. It is significant that the viscosity of the system in this range is lower when the shear stress is decreased, compared to the values as the shear stress is increased. We suspect that this effect originates in the nature of the surperbridges that form during the decrease in stress, but an unambiguous interpretation of these results is not at present possible.

The hysteresis observed when the system is stressed into the TN3 region (shear stress of 400 Pa) is even more complex, but, perhaps, somewhat easier to understand. Here the viscosity is lower as the shear stress is relaxed from 400 Pa, but a crossover occurs at ca. 120 Pa, so that at lower shear stresses the solution viscosity is higher than in the original Newtonian regime. The pronounced hysteresis reflects slow relaxation of the global structure, and the persistence of the hysteresis into the low-shear stress range implies that the relaxation of the network structure is even slower than in the case of the data presented in Figure 10b. The plateau modulus data presented in Figure 9 indicate that when the polymer solution is stressed into the TN3 region, there is a substantial breakdown of the network structure, leading to a decrease in the number of mechanically active bridges. This involves a scission of superbridges and rearrangement of the network structure into associated micelle aggregates of finite size. When the stress level is decreased, these structures begin to reassociate through loop-to-bridge transitions. The fact that the steady-shear viscosity is higher at low stress after this sample history than in the initial solution suggests that there are a larger number of mechanically active chains (a larger number of percolating structures) created by reassociation of these fragmented structures, although it is possible that a more serious rearrangement of the system has taken place.

Overview of the Molecular Behavior. On the basis of the results described above, we attempt to present an overview of the structure of the system and how it changes at different applied shear stresses. Our picture of the Newtonian regime is unchanged from that presented in Figure 1 and on the left-hand side of Figure 8: at a concentration of 2 wt %, the system consists of flower micelles, bridged aggregates of finite size and a small fraction of percolating structures that form a weak gel, all in dynamic equilibrium. Under quiescent conditions, the balance between these structures is a function

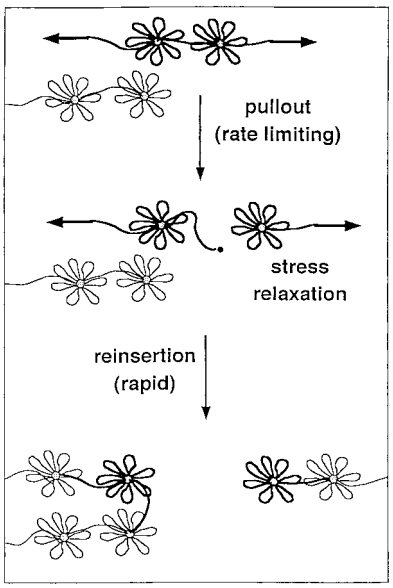

Figure 11. (a) Shear stress enhances the pullout rate of a bridging chain. (b) Stress relaxation after pullout. (c) Dangling chain end enters a new micelle forming a loop or a new bridge.

of polymer concentration. As the system is subjected to shear, the system maintains its global equilibrium structure as long as the relaxation rate is faster than the imposed shear rate.

Shear Thickening Region. Shear thickening occurs as a consequence of a shear-induced 70% increase in the plateau modulus (Figure 9). The associations are dynamic in nature, and the process is rapid. We represent this effect in Figure 8 as a corresponding increase in the density of mechanically effective chains, which comes about through an increase in the ratio of bridging to looping chains. A likely source of this increase is an incorporation of aggregates of finite size into the percolation structures of the network, leading to a net shortening of the superbridges. Shorter superbridges should lead to longer relaxation times, whereas only a small increase in λ is observed in this regime. In this regime the system also begins to experience a shear-induced increase in the chain-end exit rate from the micelle cores, which would lead to shorter relaxation times. The actual values observed in Figure 9 represent a balance between these two effects.

Shear Thinning Regions TN1 and TN2. Beyond the maximum viscosity in the shear-thickening region, a large drop in the viscosity is observed with increasing shear stress. In both the TN1 and TN2 regimes the plateau modulus remains high, and it is the relaxation time λ that is responsible for the decrease in viscosity. The data in Figure 9 indicate that when the applied stress is increased from 100 to 300 Pa, the exit rates of the hydrophobes increase by about 4 times. Thus the decrease in the viscosity in this flow regime must be associated with the disruption and rearrangement of the superbridge network junctions, but in such a way that the number of bridging chains is conserved. In Figure 11 we emphasize our view that these flow fields cannot increase significantly the concentration of free chain ends in the solution. We show that when a chain bridging two associated micelles is subjected to an applied stress, the stress is relaxed through a shear-enhanced rate of exit of one chain end from a micellar core. The dissociation step is rate-limiting, and the free chain end rapidly inserts itself into another micelle (bridge-to-bridge transition) or loops back to imbed itself in its own micelle core (bridge-to-loop transition).

An interesting feature of these experiments is that the distribution of relaxation times narrows in this regime, as seen in the $H\lambda$ vs λ curves for an applied stress of 200 Pa in Figure 7. This may indicate a more narrow distribution of superbridge lengths under these flow conditions.

In the thixotropy experiments, we find that when the stress is slowly reduced from 300 to 100 Pa, hysteresis occurs, and the viscosity over this stress region is lower than that when the stress is increased. Long relaxation times in associating polymer systems are often related to the need for multiple relaxation steps to restore the system to its original structure.[13,40] The hysteresis we observe indicates that the shear history imposed on the sample results in major changes in the global structure and that the relaxation of the system toward its equilibrium structure is slow on the experimental time scale for these experiments at shear stresses between 300 and 100 Pa. When the stress is further reduced, the original viscosity is recovered, indicating that the global structure after recovery is identical to that of the original solution.

Shear-Thinning Region TN3. At applied stresses greater than ca. 300 Pa, a large decrease in the solution viscosity is accompanied by a large decrease in the plateau modulus. The values of G_0 in this region are estimated from the expression $G_0 = \eta/\lambda$, where the values of η are obtained from the steady-shear curve (Figure 3) and the values of λ are from the oscillatory data at applied stresses of 300 and 400 Pa (Figure 4a). The reduction observed in the plateau modulus indicates that a major rearrangement of the system has occurred and suggests that there has been a significant decrease in the number of mechanically active chains. The apparent decrease in the plateau modulus in this region is rather steep: a small increase in the applied stress yields a large drop in the magnitude of G_0.

The viscosity of Maxwell fluids is dependent on two separate processes, as described by eq 10 where λ is the relaxation time and G_0 is the plateau modulus.

$$\eta = \lambda G_0 \tag{10}$$

On the basis of eq 10, the decrease in the viscosity under shear can either be a result of the reduction in the relaxation time or the number of mechanically active junctions (or increase in the fraction of loops). As shown in Figure 9, no significant reduction of G_0 is observed at the onset of shear thinning; thus the reduction in the relaxation time is mainly responsible for the shear-thinning behavior in regions TN1 and TN2. However, it is expected that the formation of loops under shear would be more significant at lower polymer concentrations, and on the basis of eq 10, it is highly probable that the viscosity decrease would be due to the reduction in λ and G_0. Studies are underway to elucidate this phenomenon.

Previous studies using fluorescence techniques have shown that the size of the micelle core under steady-shear[26] and extensional flows[27] is conserved in the region where a large drop in the viscosity is encountered. While it is not clear from these reports which of the shear-thinning regimes were monitored, we will assume for our results that the core size of the micelles is maintained during this rearrangement. Thus we infer that the reduction in G_0 is due to the fragmenta-

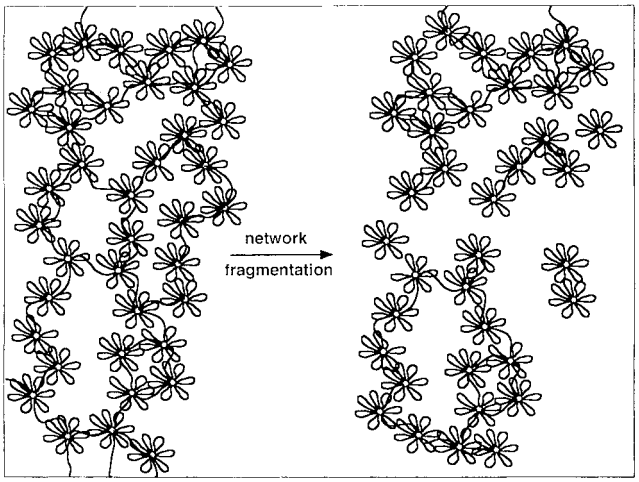

Figure 12. Structural model of the HEUR at the third shear-thinning region (TN3). The model depicts the fragmentation of the superbridges, yielding a structure with a smaller number of junctions.

tion of a significant proportion of the network chains to yield a system that has a larger fraction of finite aggregates, which do not contribute to the plateau modulus. A pictorial representation of this phenomenon is shown in Figure 12. In the thixotropy experiments, solutions subjected to a 400 Pa shear stress followed by the gradual removal of stress exhibit a pronounced hysteresis over the whole range of applied stress. Here the low-shear viscosity in the Newtonian region has increased by about 10% over its value in the fully relaxed solution. While it is difficult to interpret small effects unambiguously, it is likely that that the finite structures created in the TN3 shear-thinning regime have a higher ratio of bridging-to-looping chains than the fully relaxed system. Reassociation of these aggregates, as the shear stress is diminished, leads to structures that contain somewhat more bridges than for the system at equilibrium.

Summary

The superposition of oscillation on steady-shear experiments on a HEUR polymer solution (at 2.0 wt %) can be used to elucidate the network structure of the rosette micelles under various shear conditions. We have been able to measure the plateau modulus and the Maxwell relaxation times under these conditions, which provide information on the network junction density and the exit rate of the polymer systems, respectively. A refined structural model to describe the shear-thickening and shear-thinning region is proposed.

Acknowledgment. We wish to acknowledge the useful discussion with Dr. Tirtaatmadja. K.C.T. and M.A.W. also acknowledge the financial support of the National Science and Technology Board, Singapore, and the Ministry of Trade and Tourism, Ontario, that facilitate the collaboration between NTU and the University of Toronto.

References and Notes

(1) Jenkins, R. D. The Fundamental Thickening Mechanism of Associative Polymers in Latex Systems: A Rheological Study. Ph.D. Thesis, Lehigh University, Bethlehem, PA, 1990.
(2) Jenkins, R. D.; Silebi, C. A.; El-Aasser, M. S. *Polym. Mater. Sci. Eng.* **1989**, *61*, 629.
(3) Annable, T.; Buscall, R.; Ettelaie, R.; Whittlestone, D. *J. Rheol.* **1993**, *37*, 695.
(4) Xu, B.; Yekta, A.; Li, L.; Masoumi, Z.; Winnik, M. A. *Colloids Surf. A* **1996**, *112*, 239.
(5) Yekta, A.; Duhamel, J.; Adiwidjaja, H.; Brochard, P.; Winnik, M. A. *Langmuir* **1993**, *9*, 881.
(6) Yekta, A.; Duhamel, J.; Brochard, P.; Adiwidjaja, H.; Winnik, M. A. *Macromolecules* **1993**, *26*, 1829.
(7) (a) Alami, E.; Rawiso, M.; Isel, F.; Beinert, G.; Binana-Limbele, W.; François, J. In *Hydrophilic Polymers*; Glass, J. E., Ed.; ACS Advances in Chemistry Series 248; American Chemical Society: Washington, DC, 1996; p 343. (b) François, J.; Maitre, S.; Rawiso, M.; Sarazin, D.; Beinert, G.; Isel, F. *Colloids Surf. A* **1996**, *112*, 251.
(8) Huldén, M. *Colloids Surf. A* **1994**, *82*, 263.
(9) Semenov, A. N.; Nykrova, I. A.; Khokhlov, A. R. *Macromolecules* **1995**, *28*, 7491.
(10) Tanaka, F.; Edwards, S. F. *J. Non-Newtonian Fluids Mech.* **1992**, *43*, 247.
(11) Glass, J. E., Ed. *Hydrophilic Polymers*; ACS Advances in Chemistry Series 248, American Chemical Society: Washington, DC, 1996.
(12) Dubin, P.; Bock, J.; Davis, R.; Schulz, D. N.; Thies, C. *Macromolecular Complexes in Chemistry and Biology*; Springer-Verlag: Berlin, 1994.
(13) Groot, R. D.; Agterof, W. G. M. *Macromolecules* **1995**, *28*, 6284.
(14) Amis, E. J.; Hu, N.; Seery, T. A. P.; Hogen-Esch, T. E.; Yassini, M.; Hwang, F. In *Hydrophilic Polymers, Performance with Environmental Acceptability*; Glass, J. E., Ed.; American Chemical Society: Washington, DC, 1996; p 279.
(15) Annable, T.; Buscall, R.; Ettelaie, R. *Colloids Surf. A* **1996** *112*, 97.
(16) Yekta, A.; Xu, B.; Duhamel, J.; Adiwidjaja, H.; Winnik, M. A. *Macromolecules* **1995**, *28*, 956.
(17) Alami, E.; Almgren, M.; Brown, W. *Macromolecules* **1996**, *29*, 2229.
(18) Rao, B.; Uemura, Y.; Dyke, L.; Macdonald, P. M. *Macromolecules* **1995**, *28*, 531.
(19) Persson, K.; Abrahamsén, S.; Persson, K.; Stilbs, P.; Hansen, F. K.; Walderhaug, H. *Colloid Polym. Sci.* **1992**, *270*, 465.
(20) Walderhaug, H.; Hansen, F. K.; Abrahamsén, S.; Persson, K.; Stilbs, P. *J. Phys. Chem.* **1993**, *97*, 8336.
(21) Hansen, F. K.; Nyström, B.; Walderhaug, H. *Macromol. Symp.* **1995**, *92*, 345.
(22) Wang, Y.; Winnik, M. A. *Langmuir* **1990**, *6*, 1437.
(23) (a) Semenov, A. N.; Joanny, J. F.; Khokhlov, A. R. *Macromolecules* **1995**, *28*, 1066. (b) Borisov, O. V.; Halperin, A. *Macromolecules* **1996**, *29*, 2612.
(24) Halperin, A. *Macromolecules* **1987**, *20*, 2943.
(25) (a) Maechling-Strasser, C.; Clouet, F.; François, J. *Polymer* **1992**, *33*, 627. (b) Maechling-Strasser, C.; Clouet, F.; François, J. *Polymer* **1992**, *33*, 1021. (c) François, J. *Prog. Org. Coat.* **1994**, *24*, 67.
(26) Richey, B.; Kirk, A. B.; Eisenhart, E. K.; Fitzwater, S.; Hook, J. J. *Coatings Technol.* **1991**, *63*, 31.
(27) Vlahiotis, T. D. S. Extensional Flow Behaviour of Associative Polymer Solutions. Ph.D. Thesis, University of Toronto, 1992.
(28) Savins, J. G. *Rheol. Acta* **1967**, *7*, 87.
(29) Vrahopoulou, V.; McHugh, A. J. *J. Non-Newtonian Fluids Mech.* **1987**, *25*, 157.
(30) Ballard, M. J.; Buscall, R.; Waite, F. A. *Polymer* **1988**, *29*, 1287.
(31) Witten, T. A.; Cohen, M. H. *Macromolecules* **1985**, *18*, 1915.
(32) Tirtaatmadja, V.; Tam, K. C.; Jenkins, R. D. *Macromolecules* **1997**, *30*, 1426.
(33) (a) Honerkamp, J.; Weese, J. *Macromolecules* **1989**, *22*, 4372. (b) Honerkamp, J.; Weese, J. *Rheol. Acta* **1993**, *32*, 65. (c) Weese, J. *Comput. Phys. Commun.* **1993**, *77*, 429.
(34) Green, M. S.; Tobolsky, A. V. *J. Chem. Phys.* **1946**, *14*, 80.
(35) Rubinstein, M.; Dobrynin, A. V. *Trends Polym. Sci.* **1997**, *5*, 181.
(36) Annable, T.; Buscall, R.; Ettelaie, R.; Shepherd, P.; Whittlestone, D. *Langmuir* **1994**, *10*, 1060.
(37) Tanaka, F.; Edwards, S. F. *Macromolecules* **1992**, *25*, 1516.
(38) Andrews, E. H.; Reed, P. E. *Adv. Polym. Sci.* **1978**, *27*, 1.
(39) Groot, R. D.; Bot, A.; Agterof, W. G. M. *J. Chem. Phys.* **1996**, *104*, 9220.
(40) Xu, B.; Yekta, A.; Winnik, M. A.; Sadeghy-Dalivand, K.; James, D. F.; Jenkins, R. D.; Bassett, D. R. *Langmuir* **1997**, *13*, 6903.

MA980148R